Atmos. Chem. Phys. Discuss., 8, 21037–21088, 2008
www.atmos-chem-phys-discuss.net/8/21037/2008/

Atmospheric Chemistry and Physics Discussions

This discussion paper is/has been under review for the journal *Atmospheric Chemistry and Physics (ACP)*. Please refer to the corresponding final paper in *ACP* if available.

The impact of weather and atmospheric circulation on O_3 and PM_{10} levels at a mid-latitude site

M. Demuzere[1,2], R. M. Trigo[2], J. Vila-Guerau de Arellano[3], and N. P. M. van Lipzig[1]

[1]Earth and environmental Sciences, Celestijnenlaan 200E, 3001 Heverlee (Leuven), Katholieke Universiteit Leuven, Belgium
[2]Department of Geophysics, University of Lisbon, Centro de Geofísica da Universidade de Lisboa Fac. Ciencias, Campo Grande, Ed. C8, Piso 6, 1749-016 LISBOA, Portugal
[3]Meteorology and Air Quality Section, Wageningen University, Droevendaalsesteeg 4, P.O. Box 47, 6700 AA Wageningen, The Netherlands

Received: 22 August 2008 – Accepted: 15 October 2008 – Published: 16 December 2008

Correspondence to: M. Demuzere (matthias.demuzere@ees.kuleuven.be)

Published by Copernicus Publications on behalf of the European Geosciences Union.

Abstract

In spite of the strict EU regulations, concentrations of surface ozone and PM_{10} often exceed the pollution standards for The Netherlands and Europe. Their concentrations are controlled by (precursor) emissions, social and economic developments and a complex combination of meteorological actors. This study tackles the latter, and provides insight in the meteorological processes that play a role in O_3 and PM_{10} levels in Cabauw (The Netherlands). The relations between meteorological actors and air quality are studied on a local scale based on observations from Cabauw and are determined by a comprehensive correlation analysis and a multiple regression (MLR) analysis in 2 modes, with and without air quality variables as predictors. Furthermore, the objective Lamb Weather Type (WT) approach based on ECMWF (European Center for Medium-range Weather Forecasting) operational data is used to assess the influence of the large-scale circulation on air quality. Keeping in mind its future use in downscaling future climate scenarios for air quality purposes, special emphasis is given to an appropriate selection of the regressor variables readily available from operational meteorological forecasts or OAGCMs (Ocean-Atmosphere coupled General Circulation Models). The regression models perform satisfactory for both O_3 and PM_{10}, with an increased performance when including previous days air quality information. The lamb weather types show a seasonal distinct pattern for high (low) episodes of average O_3 and PM_{10} concentrations, and these are clear related with the meteorology-air quality correlation analysis. Although using a circulation type approach can bring some interesting physical relations forward, our analysis reveals the circulation method is limited in terms of short-term air quality forecast for both O_3 and PM_{10}. In summary, it is concluded that the use of a regression model is more promising for short-term downscaling from climate scenarios than the use of a weather type classification approach.

1 Introduction

Ground-level ozone (O_3) and particulate air pollution (PM_{10}) have been identified as two of the most important air pollutants for Europe in general (Jol and Kielland, 1997; Brunekreef and Holgate, 2002) and over the Benelux region in particular (Tulet et al., 2000). Since their adverse health effects have been observed for decades, the supervising European institutions have produced appropriate legislation and several emission reduction measures have been taken to reduce ambient air pollution (European Community, 1999; WHO, 2000, 2005). Nevertheless, levels of O_3 and PM_{10} continue to exceed frequently the target values and the long-term objectives established in EU legislation. Moreover, international literature shows that air pollution continues to threaten human health despite these emission standards (van der Wal and Janssens, 2000; Medina et al., 2004; Schlink et al., 2006).

In recent decades, typical causes of high ozone and PM_{10} pollution received ample treatment in the scientific literature. Relatively high levels of these pollutants are usually associated to the close location of high precursor emissions and as a result of industrial and societal developments. Moreover, ambient air pollution is also strongly influenced by meteorological factors, due to a complex combination of processes and influences, namely; emission, transport, chemical transformations, and removal via wet and dry processes (Seinfeld and Pandis, 1998). Thereby, weather/climate elements play a significant role in all these processes' components. On a local scale, emission (e.g., biogenic or dust emissions) may depend on climate variables such as temperature and surface wetness; (photo) chemical processes depend on temperature, humidity, solar radiation fluxes and cloudiness; the precipitation process influences wet removal. From a regional point of view, short and long-term transport depends on the magnitude of surface turbulence and on the atmospheric circulation (at the synoptic scale). This means that the distribution of pollutants is not only dependent on the spread of its emissions, but is also affected by various weather/climatic drivers (Giorgi and Meleux, 2007).

ACPD

8, 21037–21088, 2008

Over the last few decades, the effects of chemical tracers on climate change have been investigated extensively (Intergovernmental Panel on Climate Change, 2007). Conversely, comparatively less attention has been devoted to the issue of climate-change effects on air quality (Andersson and Langner, 2007a; Jacobson, 2008). However, we believe that, in order to understand the full range of atmospheric processes that govern the evolution of air quality under a changing climate, one has to understand and quantify the processes that impact on the atmospheric pollutants on a present time scale. Air quality is affected by both local (in situ) and regional scale processes on a few tens and hundreds kilometers. As current AOGCMs (Atmospheric-Ocean Coupled Global Climate Models) are only capable of resolving phenomena at the resolution of a few hundreds of kilometers, the climate change-air quality interactions are hampered. Furthermore, many chemical atmospheric elements, and particularly those with adverse impacts on human health, such as tropospheric O_3 and PM_{10}, have a lifetime in the order of some hours to days (Seinfeld and Pandis, 1998). As a result, their distribution is highly variable in space and time and is often tied to the distribution of sources (Giorgi and Meleux, 2007).

The main aim of this paper is to study the above-mentioned weather climatology-air quality relation at both the regional and local spatial scales. On the one hand, weather-air quality interactions on the local-scale are quantified based on techniques often used in short-term air quality forecasts. Thereby, the selection of an appropriate method depends on its simplicity, practical feasibility, sufficient accuracy and should be computationally inexpensive, so that it can easily be applied to output of different climate models (Semazzi, 2003). The latter rules out the use of a complex climate-air quality modelling system (in off-or online mode), a field of research that is comprehensively reviewed by Giorgi and Meleux (2007).

Many empirical prediction models have been developed to investigate the relationships between meteorological and air quality data. Numerous reports describe model results on different air quality variables and different locations from multiple linear regression (MLR) analysis (Hubbard and Cobourn, 1998; Barrero et al., 2006; Stadlober et al., 2008), nonlinear multiple regressions (Cobourn, 2007), artificial neural networks (ANN) (Gardner and Dorling, 1998; Nunnari et al., 1998; Reich et al., 1999; Benvenuto and Marani, 2000; Perez et al., 2000; Perez, 2001; Kukkonen et al., 2003; Hooyberghs et al., 2005; Papanastasiou et al., 2007), generalized additive models and fuzzy-logic-based models (Cobourn et al., 2000). Other authors compared several methods on a single dataset (from the same measurement site) or combined various approaches in order to improve the specific air pollutant forecast (Agirre-Basurko et al., 2006; Goyal et al., 2006; Al-Alawi et al., 2008). Comrie (1997) compared the potential of traditional regression and neural networks to forecast ozone pollution under different climate and ozone regimes. Model comparison statistics indicate that neural network techniques are only slightly better than regression models for daily ozone prediction. Cobourn et al. (2000) compared nonlinear regression and neural network models for ground-level ozone forecasting in Louisville (USA). They conclude that both models performed essentially the same, as measured by various errors statistics. In contrast, Gardner and Dorling (2000), concluded that significant increase in performance is possible when using MLP (multilayer preceptron) models, whereas the use of regression models are more readily interpretable in terms of the physical mechanisms between meteorological and air quality variables.

As previous research pointed out a similar performance between liner regression and neural network techniques, a stepwise multiple linear regression model is used, which also guarantees simplicity by the linear structure of the model. Practical feasibility is obtained by including these parameters that are provided/forecasted individually by OAGCMs/operational models. On the other hand, the discriminative power of a circulation classification method is tested as an air quality assessment tool, keeping in mind its potential future use in downscaling future climate scenarios for air quality purposes (Huth et al., 2008). Prior to the selection of variables for the model, a comprehensive correlation study is conducted between all meteorological and air quality variables. Afterwards, levels of O_3 and PM_{10} are reconstructed using a stepwise multiple linear regression technique and a circulation pattern approach. Finally, both method-

ACPD
8, 21037–21088, 2008

ologies results are objectively compared, with the aim of stressing their corresponding (dis-)advantages for long-term air quality assessment studies.

To the best of our knowledge, this approach has never been conducted before for the Benelux area. In fact, this integrated approach connects both atmospheric chemistry on the local scale using mast observations from Cabauw (The Netherlands) and synoptic climatology based on ECMWF operational analysis data. Although the different aspects of the methodology are widely used in their specific field of application, they are seldom compared against each other. Many authors solely used the first step in forecasting future levels of air quality variables (e.g. Oanh et al., 2005; Wise and Comrie, 2005), while many studies investigated air quality in relation to the latter (Comrie, 1992; Davies et al., 1992a,b; Cannon et al., 2002; Kassomenos et al., 2003; Bridgeman and O'Connor, 2007). An objective combination of both methodologies results in a further insight in weather-air quality related issues, and presents their corresponding (dis-)advantages for long-term air quality assessment studies.

2 Data

In order to get insight in the weather-air quality interactions on the local and regional scale, different sets of meteorological and air quality data are used and described in the following sections.

2.1 ECMWF operational data

We have extracted large-scale operational data from the ECMWF (European Centre for Medium Weather Forecast) on a 2.5×2.5° grid for the larger European Atlantic Region (20° W–35° E, 75° N–35° N). This dataset is used to determine prevailing circulation patterns at the regional scale. The data covers the 2001–2004 period, identical to the period selected to train the linear model from the Cabauw measurement station (see Sect. 2.2). For the circulation pattern approach, 12 h UTC mean sea level pressure

(MSLP) is used, while the 10 m U and V wind component [m/s], total cloud cover [0–1] and 2 m (dew point) temperature [K] are daily averaged from the 6 hourly data provided by ECMWF. Wind direction is calculated from the U and V wind component [in ° from N].

2.2 Local meteorological measurements

Previous efforts to relate air quality variable concentration data to surface meteorological variables have shown that temperature, wind speed, relative humidity, and cloud cover are the relevant variables (NRC, 1991). Other meteorological-air quality studies have found wind direction, dew point temperature, sea level pressure and precipitation useful in the modelling and forecasting of air quality variables (Gardner and Dorling, 1999; Delcloo and De Backer, 2005; Hooyberghs et al., 2005; Grivas and Chaloulakou, 2006; Andersson et al., 2007a,b; Papanastasiou et al., 2007). All of these variables (with the exception of relative humidity) are available from the Cabauw mast observations and are included in the suite of meteorological data. Barrero et al. (2006) show that relative humidity correlates significantly ($p<0.01$) with suspended particles, NO_2, SO_2 and O_3, and is therefore a possible important predictor variable for the regression analysis. Therefore, the relation between 2m air and 2m dew point temperature indicates the relative humidity. To extent our analysis, also observed shortwave downward radiation is included. An overview of all meteorological variables used is given in Table 2.

The use of several types of models for ozone prediction can be particularly sensitive to different weather-ozone regimes and measurement locations (Comrie, 1997). In order to by-pass this complexity, this study solely focuses on measured high temporal resolution data from the rural measurement station of Cabauw (The Netherlands), partially operated by the KNMI. The meteorological variables are selected for the period 2001–2006, a selection that takes into account data availability, the amount of missing data and also the availability of air quality data for the same period. A quality control was performed at the KNMI whereby quality numbers for each measured parameter are defined in the same way as in the former continuous Cabauw programme (Beljaars and Bosveld, 1997). After removal of spurious data, the 10 min measurements are averaged to daily values, in order to be able to make a connection with coarsely spatial and temporal gridded data from ECMWF operational analysis or OAGCMs. Furthermore, the list of meteorological variables is extended with the calculated 2 m daily maximum and minimum temperatures (Smith et al., 2000) (Table 2). As for the air quality variables (see Sect. 2.3), the first 4 years are used to train the regression model, while the period 2005–2006 is used to validate the model.

2.3 Air quality data

Air quality variables are investigated in order to assess their role (combined with meteorological variables) controlling the levels of the two pollutants under study. Thereby, levels of O_3 and PM_{10} correspond to the two dependent variables to be modeled, whereas NO, NO_2, SO_2 concentrations are added as independent variables explaining the variation of O_3 and PM_{10} in combination with all other meteorological variables. The air quality data was obtained from the AIRBASE database (http://air-climate.eionet.europa.eu/databases/EuroAirnet/). Hourly measurements of O_3, NO, NO_2 and SO_2 are selected from the rural background station of Cabauw, for the period 2001–2006. As PM_{10} is not available at the Cabauw site, it is selected from the neighboring station of Zegveld-Oude Meije, which has similar characteristics. Due to lack of data the PM_{10} time series is restricted to a shorter period from March 2003 until end of 2006 (Table 3). These locations are chosen with the expectation that, by selecting a rural background station, non-local correlations would be more clearly revealed and the confounding effect of local urban vehicular NO_x emissions are avoided (Gardner and Dorling, 2000). The readings for all air quality variables are performed on a regular basis, with less than 7% missing values for Ozone, NO, NO_2 and SO_2, except for PM_{10}, which has 9% missing values (Table 3). Taking into account the use of meteorological variables on a daily scale, a representative daily value is considered for each pollutant. For SO_2 and PM_{10} daily means are considered, while for O_3 the daily 8 hourly maximum mean and for NO and NO_2 the daily maximum value is used

(European Community, 1999).

The typical patterns of daily and monthly variability of O_3, NO, NO_2 and SO_2 and PM_{10} for the whole period are shown in Fig. 1. The yearly cycles of O_3 reveal the highest peak concentrations in summer, whereas for NO and NO_2, the annual cycle is characterized by a summer minimum and a maximum in winter. For SO_2 and PM_{10}, this seasonality is less pronounced, although a less distinct peak can be seen for PM_{10} in February and March. This is confirmed by the annual cycles of O_3, NO, SO_2 and PM_{10} between 1995 and 2001 presented by Flemming et al. (2005), based on hundreds of German air quality stations (see their Fig. 3).

Monthly and seasonal statistical data for Cabauw and Zegveld-Oude Meije are depicted using Box-Whisker plots (Fig. 2). For O_3 it is found that the highest median concentrations are observed in spring months (MAM), whereas peak concentrations occur in summer (JJA). This refers to the presence of a spring and summertime maximum often seen in midlatitudes (Delcloo and De Backer, 2008). As is also shown by Figs. 1 and 2, the lowest daily medians of surface ozone concentrations are found in November, December and January. For NO and NO_2, the opposite situation prevails whereby the highest concentrations can be found in winter months (November, December and January), and the lowest during June and July (Fig. 2). This is in line with Mondal et al. (2000) and Harrison et al. (1997) who have detected a similar seasonal curve for NO_x in both Calcutta and Birmingham. This mutual relation between O_3, NO and NO_2 can be understood from the photochemical ozone production in the well known sequence (Sillman, 1999):

$$HO_2 + NO \rightarrow NO_2 + OH \quad (1)$$

$$NO_2 + h\nu \rightarrow NO + O(^3P) \quad (2)$$

$$O(^3P) + O_2 + M \rightarrow O_3 + M \quad (3)$$

The oxides of nitrogen (next to CO and volatile organic compounds (VOC) which react with the hydroxyl radical OH) are precursors in the nonlinear chemical process forming O_3. In this respect, scientists have attempted to characterize local regions as

ACPD
8, 21037–21088, 2008

“NO_x-limited” and “VOC-limited” with respect to the reduction of photo-oxidant formation. The regime in a particular region will depend principally on the concentration of NO_x and the VOC/NO_x ratio. Thereby, urban areas are often denoted as “VOC-limited” (lower VOC concentrations), whereas rural and suburban areas are denoted as “NO_x-limited” (lower NO_x concentrations) (Reis et al., 2000). Hereby NO_x acts as a catalyst and produces O_3 till its removal as NO_3 by deposition processes or its conversion into other forms of nitrogen. More detailed information on the photochemical reactions forming ozone under varying NO_x and volatile organic compounds emissions can be found in Sillman and He (2002).

The O_3-NO_x interaction can, to a large extent, explain the opposite monthly behavior of O_3, NO and NO_2 in Figs. 1 and 2 (NRC, 1991; Sillman, 1999; Satsangi et al., 2004; Lasry et al., 2005). For SO_2 and PM_{10}, concentration levels are rather constant throughout the year. The highest monthly SO_2 concentrations are reached in January and June, while the maximum daily concentration is reached in March. Additionally, differences among different seasons can be considered relatively small (<1 standard deviation). For PM_{10}, maximum daily mean concentrations are found in June and December. Also for PM_{10}, seasonal differences are smaller than 1 standard deviation of monthly mean concentrations.

3 Methods

It is now widely accepted that there are two main approaches in synoptic climatology to investigate the links between local-scale environmental features and large-scale circulation patterns (Yarnal, 1993): the environmental-to-classification approach and the classification-to-environmental approach. The former lacks any capability in a predictive mode, but can be of use in a descriptive way to get more insight in those patterns that are regulating the magnitude of surface environmental variables. Therefore, we adopt the latter, which has the capability to calculate expected air quality conditions related to each circulation pattern, and to compare this forecast with the observed air quality values to evaluate the strength of the circulation-to-environmental approach (Cannon et al., 2002).

3.1 Stepwise regression analysis

Our goal is to model the maximum 8 hourly mean O_3 and mean daily PM_{10} levels by a linear model that will form the basis for our understanding and reconstruction of the air quality variables based on local-scale meteorological and air quality observations. Thereby, stepwise multiple linear regression models are conceived for both the dependent variables O_3 and PM_{10}.

First, we have assessed the linear nature of the relationship between the dependent and independent datasets. If these relations are non-linear, than an appropriate variable transformation should be applied in order to assure linearity. Secondly, the data is checked for the existence of multicollinearity. If the tolerance (a measure for the strength of a linear relationship among the independent variables) between two variables is below a threshold value of 0.1 (Norusis, 2002), than these variables are highly related and their simultaneous use can interfere with a correct interpretation of the regression results. In such a situation, the variables that suffer from multicollinearity should be identified and some of them removed from the rest of the analysis. The linear multiple regression is generally formulated as

$$Y_i = B_0 + B_1 x_{i1} + B_2 x_{i2} + \ldots + B_p x_{ip} + \varepsilon_i$$

where, for observations i, Y_i is the predictand variable,B_0 a coefficient, $B_1, B_2, \ldots, B_p$ the coefficients for p independent variables $X_1, X_2, \ldots, X_p$ (the predictors) and ε_i is the residual error (difference between the observations and the predicted values). Thereby, the observations $\{X_1, X_2, \ldots, X_p\}$ are used to estimate the parameters $B_1, B_2, \ldots, B_p$. Hence, the equation for the predicted value is:

$$\hat{Y}_i = b_0 + b_1 x_{i1} + b_2 x_{i2} + \ldots + b_p x_{ip}$$

with b_i as an estimation for B_i, and $\hat{Y}_i$ is the predicted value. The goal of the analysis is to determine the values of the parameters of the regression equation and to quantify the goodness of the fit in respect to the dependent variable Y, using the measures explained in Sect. 3.3.

3.2 Circulation-to-environmental approach

As our aim is to test the circulation patterns as a future air quality assessment tool, the circulation-to-environmental approach will be followed using the automated Lamb Weather Type classifications (hereafter called WTs) adapted from Jenkinson and Collison (1977) and Jones et al. (1993) to the Low Countries. The rationale for using this approach is that the identification of a clear link between circulation patterns and air quality variables could be used as a downscaling tool for air quality assessment, using operational analysis or OAGCM data as an input.

The WTs are developed using ECMWF SLP data and for a given day they describe the location of the high and low-pressure centers that determine the direction of the geostrophic flow. A grid with 16 points is assigned over the larger Western and Central Europe, with a central point over the Benelux, in 52.5° N and 5° E (Fig. 3). We computed a set of simple atmospheric circulation indices using sea level pressure (SLP) at 12:00 UTC in these 16 grid points, namely the direction and vorticity of geostrophic flow: southerly flow (SF), westerly flow (WF), total flow (F), southerly shear vorticity (ZS), westerly shear vorticity (ZW) and total shear vorticity (Z). A small number of empirical rules devised previously (Jones et al., 1993; Trigo and DaCamara., 2000) are then used to classify each day as one of the 27 circulation types recently developed in Demuzere et al. (2008).

3.3 Model evaluation measures

Statistical model performances will be evaluated using appropriate scalar measures and skill scores (Wilks, 1995): the Pearson correlation coefficient (R), mean square error (MSE), root mean square error (RMSE) and explained variance (EV). According

ACPD

8, 21037–21088, 2008

Impact of weather and atmospheric circulation on O_3 and PM_{10}

M. Demuzere et al.

to Murphy (1988), the skill of any given model is a measure of the relative accuracy of a model with respect to a standard reference model. Hence, the skill of any model should be interpreted as the percentage improvement over a reference or benchmark model (Wilks, 1995). The two most commonly applied reference models used in atmospheric sciences are climatology and persistence. Therefore, two skill scores based on the MSE will be used in this paper with the climatological mean (MSE_{clim}) and the persistence (MSE_{pers}) as a reference:

$$SS_c\,(\mathrm{MSE}) = \frac{\mathrm{MSE} - \mathrm{MSE}_{\mathrm{clim}}}{0 - \mathrm{MSE}_{\mathrm{clim}}} \times 100\%$$

$$SS_p\,(\mathrm{MSE}) = \frac{\mathrm{MSE} - \mathrm{MSE}_{\mathrm{pers}}}{0 - \mathrm{MSE}_{\mathrm{pers}}} \times 100\%$$

with the "0" corresponding to the accuracy level that would be achieved by a perfect model.

Furthermore, the Kruskal-wallis one-way analysis of variance is used as a non-parametric method to test the difference of O_3 and PM_{10} population medians among the weather type groups (Kruskal and Wallis, 1952). A 1% significance level is used and hereafter denoted as α_{KW} in Sect. 4.3.

4 Results and discussion

4.1 Diurnal, seasonal and annual cycles

Prior to the selection of the weather and air quality variables for the regression analysis, their mutual relations are investigated in function of time. Therefore, Pearson correlation coefficients are calculated between each of the selected air quality and meteorological variables for each month separately (and averaged over all seasons) and for the entire time series (Table 3). We have used anomalies of each variable in order to remove the annual cycle. Taking into account that our time series are just four years long, a 10-day moving average is applied before averaging the time series, in order to smooth the climatological curve. We have taken into account the serial correlation when computing the Pearson correlation values, therefore attaining more correct significance levels. Thereby, the sample size *n* is replaced by an effective sample size *neff* that returns the Pearson correlation coefficient with its respective "adjusted" level of significance (Santer et al., 2000). To investigate any time lag on the relations between air quality and meteorological variables (Kalkstein and Corrigan, 1986; Styer et al., 1995; Ziomas et al., 1995; Cheng and Lam, 2000), the meteorological values from a 6, 12, 18, 24 and 48-hour lag period are included in the analysis (not shown). Below, results are described for each air quality variable separately.

O_3 – In general, O_3 correlations are not responding differently on the different time lags. Only for the 12 and 18-hour time lag, correlations coefficients between O_3 and SWD changes from positive to negative values. This is due to daily cycle of the radiation terms at mid-latitudes, which changes from a positive sign during daytime to a negative sign at night. Correlation coefficients are strongly positive between O_3, TA002 and TA002max (0.68 and 0.74 respectively) in summer. Together with a positive correlation between O_3 and Td, this points out that a low relative humidity corresponds to higher ozone concentrations. The reverse link can be observed for winter. In fact, during summer (JJA), O_3 concentrations are negatively correlated to wind speed, with a value of –0.43, whereas this signal is positive 0.29 for winter (DJF). This dichotomy is in good agreement to the results of Davies et al. (1992), who found similar correlations between a wind speed index and O_3 concentrations measured in Cabauw for the period 1978–1988 (see their Fig. 4).

NO and NO_2 – These variables show similar characteristics, and are therefore discussed together. Similarly to what was obtained for O_3, correlations are not responding differently on different time lags, except for the radiation variables. In contrary to the positive correlation coefficients between O_3 and SWD, NO and NO_2 show a clear negative relation to this radiation variable. This is due to the fact that an increasing incoming solar radiation will favor ozone formation and thus lead to an increased NO_x consump-

ACPD
8, 21037–21088, 2008
Impact of weather and atmospheric circulation on O_3 and PM_{10}
M. Demuzere et al.

tion. Furthermore, NO_x strongly anticorrelates with wind speed for all seasons, which refers to a more limited dispersion when wind speeds are low (R between −0.28 and −0.58), and to a lesser extent to cloud cover, most probably because of the rapid removal of NO_x in aqueous cloud chemistry as HNO_3 (Graedel and Crutzen, 1993). In winter, NO_x is positively correlated with surface pressure while rain appears to be anticorrelated. This could point out the removal of NO_x from the atmosphere due to wet deposition (Graedel and Crutzen, 1993). In summer, especially NO_2 is strong positively correlated the dew point temperature and TA002max with R is respectively 0.23 and 0.42.

SO_2 – As for O_3 and NO_x, the correlation coefficient between SO_2 and the 6 h, 12 h and 18 h lag shortwave downward radiation clearly shows a diurnal cycle. In contrast to the photochemical mechanisms associated with ozone, this pattern for SO_2 is probably of an anthropogenic origin. Throughout the year, rain amount is negatively correlated with SO_2, which again refers to the removal of sulphur dioxides by wet deposition, forming H_2SO_3 (Warneck, 1998). For all months except DJF, there is a positive correlation with both air and dew point temperature. As TA002 and Td002 indicate relative humidity, it is seen in DJF that, high concentration values relate to low relative humidity. This combines with a slightly negative correlation with cloud cover for the same period. There is no clear signal between wind speeds and SO_2 throughout the year.

PM_{10} – In general, correlations between PM_{10} and meteorological variables on different time lags weaken in function of an increasing lag time. Only the correlation coefficients for both the radiation variables swap sign in the course of the year, with a peak difference in summer, when solar radiation is the highest at this mid-latitude location. Similarly to the results obtained for NO_x and SO_2, rain amount is negatively correlated with PM_{10} in winter. The response of air and dew temperature on PM_{10} varies seasonally, with the highest positive correlation coefficients during the JJA (0.38), and negative during DJF (−0.24). This is consistent with the results of van der Wal and Janssen (2000), which have found that higher PM_{10} concentrations in winter (summer) coincide with lower (higher) temperature for PM_{10} levels in The Netherlands. The significant positive correlations with T002 and Td002, especially in MAM and JJA, point out the positive relationship between relative humidity and PM_{10} levels.

In summary it is possible to state from Table 3 that wind speed is strongly negative correlated with all the pollutants, a relation that is less pronounced for SO_2. In terms of the air quality variable, NO and NO_2 correlate similar with temperature and dew point temperature. From the meteorological point of view, there are differences within seasons. Hereby, Td002 correlates negatively to NO and NO_2 in DJF, while this relation is strongly positive in MAM and JJA. Also for O_3, the correlations change from significantly negative in DJF and SON, to strong positive in JJA. Rain (duration) is in general negatively correlated with all polluters, a fact that reflects the atmospheric removal process of the pollutant due to wet deposition. For air temperature, the maximum daily temperature plays the largest role, with the highest correlation for O_3 and NO_2 in JJA, and less but still significant for MAM for O_3, NO and NO_2. Cloud cover is in general negatively correlated to all air quality variables, with the strongest negative significant correlations for O_3 in MAM and JJA and in SON for NO and NO_2. This phenomenon can be explained by the fact that cloud cover is a proxy for incoming solar radiation and air temperature, especially in summer.

Previous research introduced an arithmetic index as an additional variable in forecasting a) pollutant levels for the Athens area (Ziomas et al., 1995; Grivas and Chaloulakou, 2006), b) PM_{10} levels in the Volos (Greece) area (Papanastasiou et al., 2007) or c) PM_{10} values for Belgium (Hooybergs et al., 2005). However, in our case a weekly cycle is not well established for most pollutants with the exception of NO_x, that shows a decrease during weekends (Saturday and Sunday) (Fig. 4). The fact that the Cabauw measurement station is denominated as a rural measurement station, can explain why the day-of-the-week influence on the short-term variability is limited. Flemming et al. (2005) confirms this limited weekly variation in O_3, NO, SO_2 and PM_{10} concentrations for German rural measurement stations. Furthermore, this regime of decreasing NO_x with increasing O_3 in weekends points out that this is a NO_x limited system (Reis et al., 2000).

ACPD
8, 21037–21088, 2008

From this correlation analysis depicted, it is clear that sea level pressure plays a minor role to explain the variation in air quality variables, with a significant negative correlation between P0and O_3 in DJF and positive with NO and NO_2 in DJF and SON. Nevertheless, taking into account the relevance of SLP in previous works (Vukovich, 1995, 1998; Vukovich and Sherwell 2003), this variable is retained and its usefulness evaluated with the multiple stepwise regression. Our lag analysis also points out that the addition of time lags shorter than 1 day does not provide sufficiently additional information. Therefore, only the 1 and 2 day time lags for both meteorological and air quality variables are taken into account in the subsequent regression analysis. Finally, as mentioned before and shown in Fig. 4, a weekly cycle in air quality measurements from Cabauw is not well established; therefore, this variable is also not taken into account.

Before starting the multiple regression analysis, both the linearity between the dependent and independent and the tolerance values for multicollinearity are considered. The descriptive statistics prior to the regression analysis show non-linear behavior for rain duration. Therefore, this variable is disregarded for the stepwise regression analysis. The descriptive statistics for multicollinearity show a tolerance value below the 0.1 threshold value for the air temperatures TA002, TA002max and TA002min and the dew point temperature Td002. As the dew point temperature was taken into account as an indicator of humidity, and its relevance asserted in Table 3, it is replaced by a calculated relative humidity [%] based on the air and dew point temperature measurements following the Magnus-Tetens approximation. In summary, we have disregarded precipitation and substituted the dew point temperature for the relative humidity and, in combination with removing TA002mean, results in acceptable tolerance values for all variables (Norusis, 2002).

4.2 Stepwise multiple regression

A great deal of research has been conducted to test the capacity of (linear) multiple regression (MLR) analysis and (non-linear) neural networks for air quality prediction

ACPD

8, 21037–21088, 2008

Impact of weather and atmospheric circulation on O_3 and PM_{10}

M. Demuzere et al.

purposes based on both air quality and meteorological input. It has been shown that model errors decrease by including persistency (lag effect) of the air quality variables (Perez et al., 2000; Smith et al., 2000; Perez, 2001; Barrero et al., 2006; Grivas and Chaloulakou, 2006). The aim of this research is to develop an approach that is also useful for downscaling operational low resolution or OAGCM output data in terms of air quality assessment on the longer time scales. In this context, there is no information on the air quality data as a dependent input variable. Therefore, the regression analysis is performed for two sets of predictors: 1) without any air quality data, hereafter called MET, and 2) with the 24- and 48-h time lag values of air quality variables included as independent variables, hereafter called METCHE. An overview of all variables used in the multiple stepwise regression analysis is given in Table 4.

Multiple linear regression with a stepwise method for variable selection was used to reconstruct time series for O_3 and PM_{10} with F probability <0.05 to enter and F probability <0.10 to exit. The model was developed with the data subset covering the whole period, from 1 January 2001 to 31 December 2004. Missing data was treated following a listwise deletion (Norusis, 2002), which means that for PM_{10}, only the period from 20 March 2003 until 31 December 2004 is considered.

Table 5 shows the resulting model coefficients for both O_3 and PM_{10}. All the variables introduced in the model are associated to a coefficient that is statistically significant. For both MLR_{MET} and MLR_{METCHE}, relative humidity is the most significant variable. This is in accordance with the results of Lu et al. (2006) and Sousa et al. (2007), who found similar results respectively using MLR for the prediction of ozone in 4 locations in Taiwan and based on PCA for the region of Oporto in Portugal. Furthermore, TA002max plays an important role, both of the present and previous day in both analyses for O_3. Including air quality variables as predictors explains 15% more of the observed O_3 variance, whereby O_3 and NO_3 concentrations from the previous day provide additional relevant information in agreement with results obtained in previous studies by Davis and Speckman (1999) and Barrero et al. (2006). Both MLR_{MET} and MLR_{METCHE} also reflect the importance of shortwave downward radiation and wind speed, and for

MLR_{METCHE}, the concentrations of nitrogen oxides of the previous day.

For PM_{10}, wind speed is most significant when no air quality predictors are included while TA002max is important in both models, results that agree with those obtained by Stadtlober et al. (2008) for Bolzano (Austria). The model results improve from R^2=0.25 for MLR_{MET} to R^2=0.42 when the air quality variables are included (MLR_{METCHE}). Here, the previous day PM_{10} concentration is shown to be an important parameter for the prediction of PM_{10} levels, as was shown in previous works (e.g. Hooyberghs et al., 2005; Stadtlober et al., 2008). Furthermore, also previous day NO is in important indicator for high PM_{10} concentrations. This strong correlation indicates road traffic as a local source (Harrison et al., 1997). Although Zegveld-Oude Meije and Cabauw are classified as a background rural station, the different behavior of NO depending on the day of the week (Fig. 4) points out the influence of road traffic on the PM_{10} measurements. This tendency is confirmed by the recent results of Schaap et al. (2008), who have found higher $PM_{2.5}$ concentration in Cabauw compared to other European rural background areas. A comparison of the quality of the two models for PM_{10} shows that our results are of similar magnitude of those by Slini et al. (2006) and van der Wal and Janssen (2000), that have obtained a correlation coefficient of respectively 0.297 and 0.25 without any further information on air quality predictors. In the following Sect. 5, a more thorough validation of the MLR approach and a comparison with the circulation approach will be performed.

4.3 Circulation-to-environmental approach

The interannual variability of the 11 resulting Weather Types (WTs) is depicted in Fig. 5, showing the relative frequency of each WT averaged for each month over the period 2001–2004. The anticyclonic type is the most frequent circulation pattern throughout the year, except for the month October, which is dominated by the southwest (SW) and west (W) circulation types. Throughout the year, the relative frequency of cyclonic situations is almost constant, reaching a maximum value in August. The meridional circulation types north (N) and south (S) are rather constant throughout the year, except for a decrease of N from October to December. All WTs with a westerly component and thus originating in the Atlantic Ocean (SW [southwest], W [west], NW [northwest]) present stable relative frequencies through most of the year, although the NW regimes decline during winter and early spring. This phenomenon is counteracted by an increase of anticyclonic types between March and May, which is in agreement with the well known maximum of blocking frequencies over the Euro-Atlantic region (d'Andrea et al., 1998; Trigo et al., 2004). The remaining types with an eastern component (NE, E [east] and SE [southeast]) are the least frequent of all weather types throughout the year with the relative frequencies of E being virtually zero between May and August.

Figures 6 and 7 depict the statistical distribution of O_3 and PM_{10} according to their respective WT class. As not all weather type clusters have sufficient data, some percentile bars/outliers are missing from Fig. 7. For O_3, an insignificant explained variance (0.03) and α_{KW}>1% show a limited discriminative power over the whole year (Fig. 6). Nevertheless, the results based on seasons show some significant results. For DJF, highest concentrations can be observed in the C (Cyclonic), N, W and NW WTs. Davies et al. (1992b) obtained similar dependence for ozone with N,NW and W weather patterns in Cabauw. It is noticed that some of the latter are related to strong winds and tropopause folding mechanisms whereby ozone can be transported from the lower troposphere (Delcloo and De Backer, 2008). The lowest DJF concentrations can be found in E, SE and S directional circulation patterns. This discriminative power of the WT technique for O_3 assessment is supported by an explained variance of 0.26 and α_{KW}<1%. Lamb weather types do not succeed in explaining a great deal of the observed variance in MAM, which is also supported by an insignificant EV factor (0.05) and α_{KW}>1%. The relation between the WTs and concentration of O_3 in JJA is opposite compared to the DJF situation. Whereas in DJF the highest concentrations are found in West to North directions, in JJA they can be found in correspond East – Southeast directions. This coincides with the highest median concentrations of NO and NO_2 for the SE circulation pattern (not shown). This increased transport of NO_x in summer from the highly industrialised Ruhr area (located south-easterly) makes the atmosphere more abundant of O_3 precursors, which can, in combination with positive temperature anomalies/increased solar radiation lead to higher O_3 formation and concentrations. The SON patterns are a transitional period with changing conditions from JJA to DJF with a shift in highest concentrations from North to Easterly directions, and lower concentrations from Southeast to Southerly directions. For both JJA and SON, α_{KW}<1%, so that the medians of the O_3 and PM_{10} clustered per weather type group are significantly different.

In general, the Kruskal-Wallis test shows that the Lamb weather types are able to separate between high and low episodes of PM_{10}, with α_{KW}<1% in all seasons and over the whole year averaged. For DJF, the Box-Whisker plot shows the lowest concentrations of PM_{10} originating from Western to Northern circulation patterns, and the highest median concentrations during A and SE WTs. This is supported by the findings of van der Wal and Janssen (2000) who has obtained the highest PM_{10} levels in DJF in The Netherlands with winds prevailing from east to southeast. The explained variance is the highest (0.3) when compared to the other seasons. In MAM, the highest PM_{10} concentrations are grouped with the WTs ranging from East to South directions, which could be associated to the transport of PM_{10} from the high industrial Ruhr area. As for DJF and MAM, the highest PM_{10} levels can be found for the SE and S classes, and the lowest levels for types originating from West to Northwest. Again, this confirms the results of van der Wal and Janssen (2000) who reported higher levels of PM_{10} in JJA during dry weather condition with positive temperature anomalies, which is the case for the SE and S lamb weather types (not shown). In autumn, the explained variance is the lowest (0.21), although the highest levels of PM_{10} can again be associated with southeast to southern flow patterns.

In order to gain further insight into the physical conditions behind the WT-air quality relationships, we derive the seasonal composite pressure maps for each circulation pattern that is associated with the highest median of O_3 and PM_{10} (Figs. 8 and 9). For each season, the circulation type with the highest median of the air quality variable is identified, and the corresponding mean circulation pattern is depicted for the period 2001–2004 together with the SLP, temperature and relative humidity anomalies (computed with the normal period from 1971–2000). For O_3, the winter surface SLP composite map shows a meridional pressure gradient, with high pressure located just west of Ireland, and a low-pressure system positioned over north-eastern Europe. This implies a strong northerly circulation that is consistent with previous results of a strong correlation between high O_3 levels and strong winds in winter (Davies et al., 1992b). The anomaly maps show an enhanced positive pressure anomaly south of Iceland, and a negative anomaly east of Cabauw. These patterns also suggest strong winds and high frequencies of troughs or even cut-off lows in the vicinity of the observation station, which suggests transport of air mass from the upper troposphere (low troposphere) to the surface (Delcloo and De Backer, 2008). This could explain the higher concentrations associated with these patterns, as in non-summer months there is less opportunity for photochemical production of ozone in the boundary layer (Davies et al. 1992b).

The spring SLP maps show the Azores high pressure system extending far towards the northeast and a low located over Italy. This pattern results in a weak northwest-southeast pressure gradients and resulting winds from the northeast and a negative (positive) temperature (relative humidity) anomaly. The spring SLP anomalies indicate that the pressure gradient is slightly stronger than normal, a fact that is consistent with the positive (albeit insignificant) relation with wind speeds in spring.

The JJA composite SLP maps show a strong anticyclonic system located north of Cabauw, resulting in a weak meridional flow. This situation transports warm and dry air from east and central Europe to large parts of Western Europe promoting the appearance of a positive (negative) temperature (relative humidity) anomaly fields. This is consistent with the strong positive (negative) relation between temperature (relative humidity) that characterises high O_3 levels in summer. Pressure gradients and corresponding anomalies are generally weak, which is also consistent with the negative relationship between high O_3 levels and wind speed. These findings confirm the results of Delcloo and De Backer (2008), who have shown that high summer ozone events in

Uccle (Belgium) – which has generally similar synoptic characteristics as Cabauw – are often generated by slow moving air masses, residing over the continent. Furthermore, our results agree with those of Guicherit and Van Dop (1977), who found a similar relation in the 1970s between high ozone levels and the synoptic situation above The Netherlands. The Grosswetterlagen pattern associated with their high ozone levels events describe a closed high over Middle Europe (HM), high over Scandinavia (Hfa) or high over the North Sea – Iceland (Hna), comparable to our results using Lamb weather types.

The autumn composite SLP map exhibits a strong northwest-southeast pressure gradient, with an enhanced flow from the northeast. A positive pressure anomaly northeast of the British Isles is the highest compared to other seasons. Anomalies for temperature are negligible and relative humidity anomalies are slightly positive, which refers to a positive relation between and relative humidity in autumn, which is consistent with our explorative correlation analysis above.

For PM_{10}, high levels occur in situation where air masses are advected from the south or east. In DJF, a large anticyclonic systems covers large parts of north and Eastern Europe, associated with a high positive pressure anomaly centred west of the Norwegian coast. This results in a south-eastern flow (over the highly industrialized Ruhr area), and advection of cold continental air. This is consistent with the negative correlation of PM_{10} levels with temperature and the results obtained by van der Wal and Janssens (2000), who found similar results using PM_{10} data of 19 monitoring sites in The Netherlands (for the period 1993–1994). In MAM, this pattern is similar, although weaker, with a positive anticyclonic system over Scandinavia, and a low pressure placed over the Bay of Biscay, again advecting cold air from central Europe. In summer, pressure gradients are generally weak, with a weak negative (positive) pressure anomaly located west of Ireland (Baltic Sea) promoting the advection of warm air from the south. A result that is consistent with the positive correlation of PM_{10} levels and wind speed in JJA, confirming the results obtained by van der Wal and Janssen (2000) who stated that concentrations of PM_{10} are higher than normal during summer

ACPD
8, 21037–21088, 2008

Impact of weather and atmospheric circulation on O_3 and PM_{10}

M. Demuzere et al.

under conditions of high temperatures and dry weather. Autumn is characterised by a blocking high-pressure system over the measurement station, which results in calm, colder than normal weather over the area.

5 Validation of MLR and LWT

In the previous Sects. 4.2 and 4.3 we have derived results for the MLR and WT approaches highlighting the resemblance with similar research done for Benelux and in other regions. Here we provide an objective comparison between the results obtained with the MLR and the WT air quality assessment models, using the period 2001–2004 for calibration and 2005–2006 for validation purposes. Similar to the calibration dataset, all variables are transformed by removing the climatological mean as described in Sect. 4.1. For MLR, the regressions obtained in Sect. 4.2 are used on the validation dataset while for the WT methodology, O_3 and PM_{10} means are computed for each of the circulation patterns for 2005–2006. The average value of the air quality variable associated with each circulation pattern is used to reconstruct the time series.

The results of the models for both the calibration and validation periods are shown in Table 6 In general, MLR techniques are known to underestimate peak levels of ozone (Barrero et al., 2006). Although the MLR model is built from the calibration dataset, we can observe an increase in accuracy for O_3 (>10% in explained variance) when the model is applied over the validation dataset for both MLR_{MET} and MLR_{METCHE}. Thus, errors between observed and modelled O_3 levels from the validation period decrease (while EV increases), especially in JJA and DJF with 15% and 30% respectively. In terms of seasonal differences, the regression models explain more of the observed variance in DJF and JJA and less in the transition seasons. The skill score against the climatological mean is higher than 90% for both MLR_{MET} and MLR_{METCHE}, which points out that a forecast based on climatology is easily outperformed by a linear model (or an analysis based on circulation patterns). Persistence is a more difficult to beat benchmark model, therefore any positive values of SSp are particularly relevant. The better quality of the MLR_{METCHE} model when compared with the MLR_{MET} can be observed in this assessment against persistence, with an improved skill score from 36 to 50% (validation period) and from 9.9 to 27% (validation period) for MLR_{MET} and MLR_{METCHE} respectively.

Table 6 also reveals an improvement for the WT approach applied on the validation dataset compared to the calibration dataset. In general, the circulation patterns explain less than 21% of the observed O_3 variance, again with the highest scores being observed in DJF and JJA. Explained variance improves significantly (between 10 to 16%) for the WT based on seasonal means compared to yearly averages. However, overall scores are considerably lower when compared to those obtained with MLR while the RMSE values are about 5 $\mu g/m^3$ higher compared to those from the regression analysis. Although WT presents a good skill score against the climatological mean, it fails to show any significant improvement against persistence, revealing sometimes a lower quality when compared to the persistence model. This results implies that, although circulation patterns are able to discriminate between high (low) concentrations for different seasons and WTs, day-to-day variability and the complex sequence of physic-chemical ozone formation/destruction mechanisms play a large role that can not be fully captured by the circulation pattern classification.

For PM_{10}, the performance of the model increased, for MLR_{MET} model, with an EV increase of 25 and 35% for the calibration and the validation period respectively. However, the MLR_{METCHE} reveals a slight decrease from 42% to 36% between these two datasets. In general, the overall best performance based on the EV is obtained in MAM, JJA and SON, depending if the air quality variables are included as predictors or not. Results are worse for DJF, which could be due to possible high PM_{10} events related to an increased surface stability (surface inversion) that is not captured by MLR trained with surface meteorological data. The skill score for the calibration and validation dataset against climatology improves 15% for both periods, between the MLR_{MET} and MLR_{METCHE}. The skill score against persistence improves similarly for the calibration dataset, although this is not the case for the validation dataset.

ACPD
8, 21037–21088, 2008

The analysis for the PM_{10}-LWT approach shows low coefficients for the EV, although somewhat higher compared to the EV obtained for the O_3-LWT model, with a maximum explained variance for the validation period using LWT based on seasonal averages (R^2=23.29). Identical to MLR, the observed variance for PM_{10} is explained the most in MAM, and JJA. The skill score against climatology is higher for both the calibration and validation dataset compared to the MLR_{MET}, with overall high scores (>80%). For the calibration dataset, the LWT approach is performing slightly better than the persistence model, while for the validation dataset, results are worse.

Concerning the WT classification method it is fair to state that our results partially contradict previous studies that discussed the strength of synoptic categories in relation with air pollution concentrations (Comrie and Yarnal, 1992; Davies et al., 1992b; Kalkstein et al., 1996; Cheng and Lam, 2000; Ainslie and Styen, 2007). This discrepancy could be due to multiple reasons. However, we firmly believe that the most important reason is associated with the lack of validation measures used in those studies, in fact these studies described synoptic situations associated with characteristic levels of an air quality variable without objectively quantifying this result. Nevertheless other issues may also intervene, namely levels of air pollutants associated with typical circulation patterns are solely compared to other classification approaches (Cannon et al., 2002). Furthermore, there are many different classifications techniques of atmospheric circulation types (PCA, clustering, etc) taking into account a different number of variables on various pressure levels (Huth et al., 2008) and their use could alter our findings to a certain degree. In summary, our statistical analysis reveals that the single use of a weather type approach is limited in terms of short-term day-to-day air quality forecasts. Nevertheless, our analysis also shows that a circulation type approach brings forward some interesting physical relations between large-scale circulation patterns and associated air quality concentrations. This supports the use of this approach with respect to future long-term air quality projections and low temporal air quality fluctuations, as was recently successfully tested for PM_{10} at several Bavarian sites in Germany (C. Beck, personal communication, 2008).

6 Summary and conclusion

We investigate the relationships of climatology and air quality by statistically analyzing meteorological and air quality variables calculated and observed at Cabauw (The Netherlands). On the one hand, interactions between meteorology and O_3 and PM_{10} on the local-scale are quantified based on a multiple linear regression analysis, a technique often used in short-term air quality forecasts. On the other hand, the Lamb weather type circulation classification method is applied as an alternative air quality prediction tool. This technique is potentially useful as downscaling tool of future climate scenarios for local air quality purposes.

By selecting these methods, we seek simplicity, linearity and practical feasibility of the models in order to make this approach appropriate for downscaling forecasted meteorological fields or OAGCMs scenarios for air quality purposes. The multiple linear regression model guarantees simplicity, and applying the regression without (MLR_{MET}) or with air quality variables (MLR_{METCHE}) as predictors, provides a comprehensive summary on the capabilities of these 2 modes. Comparing the results of this local-meteorology based approach with results from a circulation point-of-view based on mean sea level pressure, which takes into account the large-scale circulation above our area of interest, provides further insight in the controlling processes forming and resulting in representative O_3 and PM_{10} levels for the rural background station of Cabauw.

Prior to the construction of the multiple regression models, a comprehensive correlation study is conducted between all meteorological and air quality variables. The dataset is hereby extended including all meteorological variables on a 6, 12, 18, 24 and 48-hour time lag, in order to investigate any lagged effect on the meteorological-air quality relations. In general, this analysis shows a limited response of the air quality variables on the <1-day lag meteorological variables, apart from the inverse relations with downward solar radiation, explaining the day and night cycle. Furthermore, a clear relation is found between O_3 and (maximum) temperature in JJA, combined with a low relative humidity. NO_x is strong positively correlated with the dew point temperature

ACPD
8, 21037–21088, 2008

Title Page
Abstract Introduction
Conclusions References
Tables Figures
◀◀ ▶▶
◀ ▶
Back Close
Full Screen / Esc
Printer-friendly Version
Interactive Discussion

and 2m air temperature in JJA and is anti-correlated to cloud cover in DJF, this because of the rapid removal of NO_x in aqueous cloud chemistry as HNO_3. Rain amount is negatively correlated with NO_x, SO_2 and PM_{10} in winter, which could point out atmospheric removal due to wet deposition. Wind speed is strongly negative correlated with all the pollutants for large parts of the year, a relation that is less pronounced for SO_2.

Secondly, both multiple linear regression modes provide suitable results for the forecasting O_3 and PM_{10} for Cabauw, outperforming both climatology and persistence models. The input variables are selected in the way that they are available from operational forecast or OAGCM output (for the MET mode) and the simple and transparent character of the model provides clear insight in the importance of the specific variables that govern the evolution of O_3 and PM_{10}. The statistical performance is good in comparison to similar studies for both the calibration and the validation period, testing the 2 modes MLR_{MET} and MLR_{METCHE}. In general, including information on the previous days air quality variables improves the explained variance with 10 to 18% for ozone and PM_{10} respectively, with the best results for MLR_{METCHE} for PM_{10} in the calibration period (0.42), and for ozone using MLR_{METCHE} in the validation period (0.62). Moreover, this performance is promising when considering the skill scores against persistence, with an improvement of almost 20% for some model situations.

In order to obtain a deeper understanding of the linear relations obtained, levels of O_3 and PM_{10} are connected to large-scale circulation patterns using the objective Lamb weather type approach. Based on 12:00 UTC operational ECMWF MLSP, 11 circulation types are obtained, which are on a seasonal and annual scale associated with levels of O_3 and PM_{10}. As was elaborated in previous research, some clear physicals links can be seen between the large-scale patterns and high (low) pollution events. In general, all relations between pressure, wind speed, temperature and relative humidity and levels of O_3 and PM_{10} found in our correlation coefficient analysis using mast observations from Cabauw can be retrieved from the seasonal composite circulation patterns and their anomalies. For O_3, the surface pressure composite maps generally show an anomalous strong high north or west from the measurement station, depending on the season. This results in cold and humid (DJF and MAM) and warm and dry (JJA) air advected from north to east wind directions, contributing to higher than normal ozone concentrations. Using the circulation patterns for ozone in winter reveals the highest average concentration in wind direction from W to N, under high wind speed circumstances. This feature suggests the influence of ozone transported from the free troposphere towards the surface, which was also suggested by Davies et al. (1992b) and Delcloo and De Backer (2008). For PM_{10}, high levels are overall controlled by air advected from the south to east. Hereby, pressure gradients are often low, with a positive pressure anomaly north- to eastwards from the measurement station, again depending on the season.

Finally, reconstructing the time series of O_3 and PM_{10} for the calibration and validation period objectively compares the multiple stepwise regressions and the objective Lamb weather type approach. Although the explained variance and the skill score against climatology is high (>80%), the results against persistence often point out the weakness of the model. Thereby, the stepwise regression for O_3 performs satisfactory for all indices. Contrarily, although seasonal composite maps have shown a distinct pattern for typical episodes of high average O_3 and PM_{10} concentrations, the Lamb weather type as an air quality forecast model performs poor for both O_3 and PM_{10}, whereby the skill score against persistence is, in some situations, even worse than persistence itself. On the one hand, this result could be due to the short time availability of the air quality data, which restrains the possibility to obtain a robust dataset with significant within-season and type-associated differences in concentrations of O_3 and PM_{10}. On the other hand, this result points out the limitation of the circulation-based approach in terms of day-to-day air quality forecasts. Although circulation patterns can provide a clear insight in typical large-scale atmospheric structures and associated anomalies in meteorological variables during high (or low) pollution events, this approach is not able to capture short- term fluctuations of the pollutants, which is to be expected from the intrinsic nature of the circulation. Further research could provide more insight in the possible adaptation of the multiple regression results on OAGCM output, the use of circulation pattern in providing possible long-term trends of a specific air quality variable, and on the use of a combination of a multiple regression and circulation-type approach. Thereby, O_3 and PM_{10} levels could be explained using the multiple regression technique for the local-scale photochemical formation and the circulation-based approach for the large-scale transport of (secondary) pollutants from other source areas.

Acknowledgements. This research is funded by a PhD grant of the Institute for the Promotion of Innovation through Science and Technology Flanders. The authors are especially thankful to the COST Office and the constructive discussions in the framework of COST action 733 on Harmonization and Applications of weather types Classifications for European Regions. ECMWF is acknowledged for providing operational ECMWF data. Furthermore I would like to thank some specific persons: Fred Bosveld from KNMI in providing the Cabauw mast observations; Hans Berkhout (RIVM) for his helpful insight information on the air quality measurements and locations; Karen Van de Vel (VITO), for her useful comments on atmospheric-chemistry processes.

References

Agirre-Basurko, E., Ibarra-Berastegi, G., and Madariaga, I.: Regression and multilayer perceptron-based models to forecast hourly O-3 and NO2 levels in the Bilbao area, Environ. Modell. Softw., 21, 430–446, 2006.

Ainslie, B. and Steyn, D. G.: Spatiotemporal trends in episodic ozone pollution in the Lower Fraser Valley, British Columbia, in relation to mesoscale atmospheric circulation patterns and emissions, J. Appl. Meteorol. Clim., 46, 1631–1644, 2007.

Al-Alawi, S. M., Abdul-Wahab, S. A., and Bakheit, C. S.: Combining principal component regression and artificial neural networks for more accurate predictions of ground-level ozone, Environ. Modell. Softw., 23, 396–403, 2008.

Andersson, C. and Langner, J.: Inter-anual variations of ozone and nitrogen dioxide over europe during 1958–2003 simulated with a regional CTM, Water Air Soil Poll., 7, 15–23, 2007a.

Andersson, C., Langner, J., and Bergström, R.: Interannual variation and trends in air pollu-

tion over Europe due to climate variability during 1958–2001 simulated with a regional CTM coupled to the ERA40 reanalysis, Tellus A, 59B, 77–98, 2007b.
Barrero, M. A., Grimalt, J. O., and Canton, L.: Prediction of daily ozone concentration maxima in the urban atmosphere, Chemometr. Intell. Lab., 80, 67–76, 2006.
Beljaars, A. C. M. and Bosveld, F. C.: Cabauw data for the validation of land surface parameterization schemes, J. Climate, 10, 1172–1193, 1997.
Benvenuto, F. and Marani, A.: Nowcasting of urban air pollutants by neural networks, Nuovo Cimento C, 23, 567–586, 2000.
Bridgeman, H. and O'Connor, J.: Relationships between air pollution and meteorology in Newcastle, Australia, in: Proceedings of the 6th International Conference on Urban Air Quality, 2007.
Brunekreef, B. and Holgate, S. T.: Air pollution and health, Lancet, 360, 1233–1242, 2002.
Cannon, A. J., Whitfield, P. H., and Lord, E. R.: Synoptic map-pattern classification using recursive partitioning and principal component analysis, Mon. Weather Rev., 130, 1187–1206, 2002.
Cheng, S. Q. and Lam, K. C.; Synoptic typing and its application to the assessment of climatic impact on concentrations of sulfur dioxide and nitrogen oxides in Hong Kong, Atmos. Environ., 34, 585–594, 2000.
Cobourn, W. G., Dolcine, L., French, M., and Hubbard, M. C.: A comparison of nonlinear regression and neural network models for ground-level ozone forecasting, J. Air Waste Manag., 50, 1999–2009, 2000.
Cobourn, W. G.: Accuracy and reliability of an automated air quality forecast system for ozone in seven Kentucky metropolitan areas, Atmos. Environ., 41, 5863–5875, 2007.
Comrie, A. C.: An enhanced synoptic climatology of ozone using a sequencing technique, Phys. Geogr., 13, 53–65, 1992.
Comrie, A. C. and Yarnal, B.: Relationships between synoptic-scale atmospheric circulation and ozone concentrations in Metropolitan Pittsburgh, Pennsylvania, Atmos. Environ. B-Urb., 26, 301–312, 1992.
Comrie, A. C.: Comparing neural networks and regression models for ozone forecasting, J. Air Waste Manage., 47, 653–663, 1997.
D'Andrea, F., Tibaldi, S., Blackburn, M., Boer, G., Deque, M., Dix, M. R., Dugas, B., Ferranti, L., Iwasaki, T., Kitoh, A., Pope, V., Randall, D., Roeckner, E., Straus, D., Stern, W., Van den Dool, H., and Williamson, D.: Northern Hemisphere atmospheric blocking as simulated

by 15 atmospheric general circulation models in the period 1979–1988, Clim. Dynam., 14, 385–407, 1998.

Davies, T. D., Kelly, P. M., Low, P. S., and Pierce, C. E.: Surface ozone concentrations in Europe – Links with the regional-scale atmospheric circulation, J. Geophys. Res.-Atmos., 97, 9819–9832, 1992a.

Davies, T. D., Farmer, G., Kelly, P. M., Glover, G. M., Apsimon, H. M., and Barthelmie, R. J.: Surface pressure pattern indicators of mean monthly pollutant concentrations in southern scandinavian precipitation – a test using case-studies of months with high and low concentrations of nonmarine sulfate and nitrate, Atmos. Environ. A-Gen., 26, 261–278, 1992b.

Davis, J. M. and Speckman, P.: A model for predicting maximum and 8 h average ozone in Houston. Atmos. Environ., 33, 2487–2500, 1999.

Delcloo, A. W. and De Backer, H.: Modelling planetary boundary layer ozone, using meteorological parameters at Uccle and Payerne, Atmos. Environ., 39, 5067–5077, 2005.

Delcloo, A. W. and De Backer, H.: Five day 3-D back trajectory clusters and trends analysis of the Uccle ozone sounding time series in the lower troposphere (1969–2001), Atmos. Environ., 42, 4419–4432, 2008.

Demuzere, M., Werner, M., Van Lipzig, N.P.M, Roeckner, E.: An analysis of present and future ECHAM5 pressure fields using a classification of circulation patterns, Int. J. Climatol., on press, 2008.

European Community: Council Directive 1999/39/EC of 22 April 1999 regulating to limit values for sulphur dioxide, nitrogen dioxide and oxides of nitrogen, particulate matter and lead in ambient air, Official Journal of the European Communities, L163, 0041–0060, 1999.

Flemming, J., Stern, R., and Yamartino, R. J.: A new air quality regime classification scheme for O_3, NO_2, SO_2 and PM_{10} observations sites, Atmos. Environ., 39, 6121–6129, 2005.

Gardner, M. W. and Dorling, S. R.: Artificial neural networks (the multilayer perceptron) – A review of applications in the atmospheric sciences, Atmos. Environ., 32, 2627–2636, 1998.

Gardner, M. W. and Dorling, S. R.: Neural network modelling and prediction of hourly NO_x and NO_2 concentrations in urban air in London, Atmos. Environ., 33, 709–719, 1999.

Gardner, M. W. and Dorling, S. R.: Meteorologically adjusted trends in UK daily maximum surface ozone concentrations, Atmos. Environ., 34, 171–176, 2000.

Giorgi, F. and Meleux, F.: Modelling the regional effects of climate change on air quality, C. R. Geosci., 339, 721–733, 2007.

Goyal, P., Chan, A. T. and Jaiswal, N.: Statistical models for the prediction of respirable sus-

pended particulate matter in urban cities, Atmos. Environ., 40, 2068–2077, 2006.
Graedel, T. E. and Crutzen, P. J.: Atmospheric Change: An Earth System Prospective, Freeman, New York, 1993.
Grivas, G. and Chaloulakou, A.: Artificial neural network models for prediction of PM_{10} hourly concentrations, in the greater area of Athens, Greece, Atmos. Environ., 40, 1216–1229, 2006.
Guicherit, R. and Van Dop, H.: Photochemical production of ozone in western Europe (1971–1975) and its relation to meteorology, Atmos. Environ., 11, 145–155, 1977.
Harrison, R. M., Deacon, A. R., Jones, M. R., and Appleby, R. S.: Sources and processes affecting concentrations of PM_{10} and $PM_{2.5}$ particulate matter in Birmingham (UK), Atmos. Environ., 31, 4103–4117, 1997.
Hooyberghs, J., Mensink, C., Dumont, G., Fierens, F., and Brasseur, O.: A neural network forecast for daily average PM_{10} concentrations in Belgium, Atmos. Environ., 39, 3279–3289, 2005.
Hubbard, M. C. and Cobourn, W. G.: Development of a regression model to forecast ground-level ozone concentration in Louisville, KY, Atmos. Environ., 32, 2637–2647, 1998.
Huth, R., Beck, C., Philipp, A. Demuzere, M. Ustrnul, Z., Cahynova, M., Kysely, K., and Tveito, O. E.: Classifications of atmospheric circulation patterns: recent advances and applications, [in Trends and Directions in Climate Research], Ann. N.Y. Acad. Sci., 1146, 105–152, 2008.
Intergovernmental Panel on Climate Change (IPCC): the Physical Science Basis, Contribution of Working Group I to the Fourth Assessment Report of the IPCC, 2007: http://www.ipcc.ch, last access: 20 July 2008, 2007.
Jacobson, M. Z.: On the causal link between carbon dioxide and air pollution mortality, Geophys. Res. Lett., 35, 1–5, 2008.
Jenkinson, A. F. and Collison, B. P.: An initial climatology of gales of the North Sea, Synoptic Climatology Branch Memorandum 62, 1977.
Jol, A. and Kielland, G.: Air Pollution in Europe 1997, European Environment Agency, Copenhagen, 1997.
Jones, P. D., Hulme, M., and Briffa, K. R.: A comparison of lamb circulation types with an objective classification scheme, Int. J. Climatol., 13, 655–663, 1993.
Kalkstein, L. S. and Corrigan, P.: A synoptic climatological approach for geographical analysis: assessment of sulfur dioxide concentrations, Ann. Assoc. Am. Geogr., 76, 381–395, 1986.
Kalkstein, L. S., Nichols, M. C., Barthel, C. D., and Greene, J. S.: A new spatial synoptic

classification: Application to air-mass analysis, Int. J. Climatol., 16, 983–1004, 1996.
Kassomenos, P. A., Sindosi, O. A., Lolis, C. J., and Chaloulakou, A.: On the relation between seasonal synoptic circulation types and spatial air quality characteristics in Athens, Greece, J. Air Waste Manage., 53, 309–324, 2003.
Kruskal, H. and Wallis, W. A.: Use of ranks in one-criterion variance analysis, J. Am. Stat. Assoc., 47, 583–621, 1952.
Kukkonen, J., Partanen, L., Karppinen, A., Ruuskanen, J., Junninen, H., Kolehmainen, M., Niska, H., Dorling, S., Chatterton, T., Foxall, R., and Cawley, G.: Extensive evaluation of neural network models for the prediction of NO_2 and PM_{10} concentrations, compared with a deterministic modelling system and measurements in central Helsinki, Atmos. Environ., 37, 4539–4550, 2003.
Lasry, F., Coll, I., and Buisson, E.: An insight into the formation of severe ozone episodes: modeling the 21/03/01 event in the ESCOMPTE region, Atmos. Res., 74, 191–215, 2005.
Lu, H. C., Hsieh, J. C., and Chang, T. S.: Prediction of daily maximum ozone concentrations from meteorological conditions using a two-stage neural network, Atmos. Res., 81, 124–139, 2006.
Medina, S., Plasencia, A., Ballester, F., Mucke, H. G., and Schwartz, J.: Apheis: public health impact of PM10 in 19 European cities, Journal of Epidemiology and Community Health, 58, 831–836, 2004.
Mondal, R., Sen, G. K., Chatterjee, M., Sen, B. K., and Sen, S.: Ground-level concentration of nitrogen oxides (NO_x) at some traffic intersection points in Calcutta, Atmos. Environ., 34, 629–633, 2000.
Norusis, M. J.: SPSS 11.0 Guide to Data Analysis, Upper saddle River, NJ: Prentice Hall, 2002.
NRC: Human Exposure Assessment for Airborne Pollution: Advances and Opportunities, National Acadamy Press, Washington DC, 1991.
Murphy, A. H.: Skill scores based on the mean square error and their relationship to the correlation coefficient, Mon. Weather Rev., 116, 2417–2424, 1988.
Nunnari, G., Nucifora, A. F. M., and Randieri, C.: The application of neural techniques to the modelling of time-series of atmospheric pollution data, Ecol. Model., 111, 187–205, 1998.
Oanh, N. T. K., Chutimon, P., Ekbordin, W., and Supat, W.: Meteorological pattern classification and application for forecasting air pollution episode potential in a mountain-valley area, Atmos. Environ., 39, 1211–1225, 2005.

Papanastasiou, D. K., Melas, D., and Kioutsioukis, I.: Development and assessment of neural network and multiple regression models in order to predict PM_{10} levels in a medium-sized mediterranean city, Water Air Soil Poll., 182, 325–334, 2007.

Perez, P., Trier, A., and Reyes, J.: Prediction of $PM_{2.5}$ concentrations several hours in advance using neural networks in Santiago, Chile, Atmos. Environ., 34, 1189–1196, 2000.

Perez, P.: Prediction of sulfur dioxide concentrations at a site near downtown Santiago, Chile, Atmos. Environ., 35, 4929–4935, 2001.

Reich, S. L., Gomez, D. R., and Dawidowski, L. E.: Artificial neural network for the identification of unknown air pollution sources, Atmos. Environ., 33, 3045–3052, 1999.

Reis, S., Simpson, D., Friedrich, R., Jonson, J. E., Unger, S., and Obermeier, A.: Road traffic emissions – predictions of future contributions to regional ozone levels in Europe, Atmos. Environ., 34, 4701–4710, 2000.

Santer, B. D., Wigley, T. M. L., Boyle, J. S., Gaffen, D. J., Hnilo, J. J., Nychka, D., Parker, D. E., and Taylor, K. E.: Statistical significance of trends and trend differences in layer-average atmospheric temperature time series, J. Geophys. Res.-Atmos., 105, 7337–7356, 2000.

Satsangi, G. S., Lakhani, A., Kulshrestha, P. R., and Taneja, A.: Seasonal and diurnal variation of surface ozone and a preliminary analysis of exceedance of its critical levels at a semi-arid site in India, J. Atmos. Chem., 47, 271–286, 2004.

Schaap, M., Apituley, A., Koelemeijer, R. B. A., Timmermans, R. M. A., Schoemaker, R., Mathijssen, J., de Leeuw, G.: On the relation between aerosolo optical depth and $PM_{2.5}$ in the Netherlands, SATLINK final report, Report 555034003, AH Bilthoven, 2008.

Schlink, U., Herbarth, O., Richter, M., Dorling, S., Nunnari, G., Cawley, G., and Pelikan, E.: Statistical models to assess the health effects and to forecast ground-level ozone, Environ. Modell. Softw., 21, 547–558, 2006.

Seinfeld, J. H. and Pandis, S. N.: Atmospheric Chemistry and Physics from Air Pollution to Climate Change, John Wiley & Sons, Inc, New York, 1998.

Semazzi, F.: Air quality research: perspective from climate change modelling research, Environ. Int., 29, 253–261, 2003.

Sillman, S.: The relation between ozone, NO_x and hydrocarbons in urban and polluted rural environments, Atmos. Environ., 33, 1821–1845, 1999.

Sillman, S. and He, D. Y.: Some theoretical results concerning O-3-NO_x-VOC chemistry and NO_x-VOC indicators, J. Geophys. Res.-Atmos., 107, 26–41, 2002.

Smith, R. L., Davis, J. M., Sacks, J., Speckman, P., and Styer, P.: Regression models for air

ACPD

8, 21037–21088, 2008

Impact of weather and atmospheric circulation on O_3 and PM_{10}

M. Demuzere et al.

pollution and daily mortality: analysis of data from Birmingham, Alabama, Environmetrics, 11, 719–743, 2000.
Slini, T., Kaprara, A., Karatzas, K., and Moussiopoulos, N.: PM_{10} forecasting for Thessaloniki, Greece, Environ. Modell. Softw., 21, 559–565, 2006.
Stadlober, E., Hormann, S., and Pfeiler, B.: Quality and performance of a PM_{10} daily forecasting model, Atmos. Environ., 42, 1098–1109, 2008.
Styer, P., Mcmillan, N., Gao, F., Davis, J., and Sacks, J.: Effect of outdoor airborne particulate matter on daily death counts, Environ. Health Persp., 103, 490–497, 1995.
Sousa, S. I. V., Martins, F. G., Alvim-Ferraz, M. C. M., and Pereira, M. C.: Multiple linear regression and artificial neural networks based on principal components to predict ozone concentrations, Environ. Modell. Softw., 22, 97–103, 2007.
Trigo, R. M. and DaCamara, C. C.: Circulation weather types and their influence on the precipitation regime in Portugal, Int. J. Climatol., 20, 1559–1581, 2000.
Trigo, R. M., Trigo, I. F., DaCamara, C. C., and Osborn, T. J.: Climate impact of the European winter blocking episodes from the NCEP/NCAR reanalyses, Clim. Dynam., 23, 17–28, 2004.
Tulet, P., Crassier, V., and Rosset, R.: Air pollution modelling at a regional scale, Environ. Modell. Softw., 15, 693–701, 2000.
van der Wal, J. T. and Janssen, L. H. J. M.: Analysis of spatial and temporal variations of PM_{10} concentrations in the Netherlands using Kalman filtering, Atmos. Environ., 34, 3675–3687, 2000.
Vukovich, F. M.: Regional-scale boundary-layer ozone variations in the Eastern United-States and their association with meteorological variations, Atmos. Environ., 29, 2259–2273, 1995.
Vukovich, F. M.: Aspects of subregional ozone variations in the SOS region, Atmos. Environ., 32, 3881–3889, 1998.
Vukovich, F. M. and Sherwell, J.: An examination of the relationship between certain meteorological parameters and surface ozone variations in the Baltimore-Washington corridor, Atmos. Environ., 37, 971–981, 2003.
Warneck P.: Chemistry of the natural atmosphere, in: International Geophysics Series, 71, 2nd ed., Academic Press, New York, 1998.
Wilks, D. S.: Statistical Methods in the Atmospheric Sciences, Academic Press, San Diego, 1995.
Wise, E. K. and Comrie, A. C.: Meteorologically adjusted urban air quality trends in the Southwestern United States, Atmos. Environ., 39, 2969–2980, 2005.

WHO: Air quality guidelines for Europe, 2nd ed. Copenhagen, World Health Organization Regional Office for Europe, 2000 (WHO Regional Publications, European Series No. 91), 2000.
WHO: World Health Organisation air quality guidelines for particulate matter, ozone, nitrogen dioxide and sulfur dioxide, global update 2005, Summary of risk assessment, World Health Organization Regional Office for Europe, 2005.
Yarnal, B.: Synoptic Climatology in Environmental Analysis, London, Belhaven Press, 1993.
Ziomas, I. C., Melas, D., Zerefos, C. S., Bais, A. F., and Paliatsos, A. G.: Forecasting peak pollutant levels from meteorological variables, Atmos. Environ., 29, 3703–3711, 1995.

Table 1. Summary of local meteorological parameters from the Cabauw measurement station.

Parameter *Measured*	Code	Unit	Height (m)	Frequency	% Miss.
Surface Pressure	P0	hPa		10 min	3%
Rain	Rain	mm		10 min	3%
Rain Duration	Rdur	s		10 min	3%
Shortwave downward Radiation	SWD	W/m^2	1.5	10 min	1%
2 m Air temperature	TA002	˚C	2	10 min	1%
2 m Dew point temperature	TD002	˚C	2	10 min	3%
Wind speed	F010	m/s	10	10 min	1%
Wind Direction	D010	°	10	10 min	1%
Cloud cover	N260	Octas (0–8)		10 min	0%
Calculated					
Maximum daily 2 m Air temperature	TA002max	˚C	2	Daily	–
Minimum daily 2 m Air Temperature	TA002min	˚C	2	Daily	–

ACPD
8, 21037–21088, 2008

Table 2. Characteristics of the air quality measurement sites in The Netherlands for the period 2001–2006, taken from the AIRBASE database.

Location	Code	Type of station	Type of area	Lat	Lon	Air quality parameter	Freq.	% Missing
Cabauw (Zijdeweg) NL0209A	620	background	rural	51°58′17″	4°55′35″	O_3	hourly	8%
						NO	hourly	5%
						NO_2	hourly	5%
						SO_2	hourly	6%
Zegveld (Oude Meije)* NL0229A	633	background	rural	52°08′20″	4°50′18″	PM_{10}	hourly	9%

* This data is only available for the period March 2003 until 31 December 2006.

ACPD

8, 21037–21088, 2008

Impact of weather and atmospheric circulation on O_3 and PM_{10}

M. Demuzere et al.

Table 3. Summary of the Pearson correlation coefficients between all daily air quality and meteorological variable anomalies, for each season separately. Correlation coefficients significant on the 99% level are depicted in bold, whereby autocorrelation effects are taken into account. Meteorological variables abbreviations are denoted in Table 1.

		O_3	NO	NO_2	SO_2	PM_{10}
P0	DJF	–0.3762	0.3467	0.3683	0.0637	0.2321
	MAM	0.1542	0.1443	0.1515	−0.0222	0.011
	JJA	0.0894	0.104	0.0585	0.0735	−0.0992
	SON	−0.0343	0.2959	0.2277	0.0831	0.0069
	YEAR	−0.0473	*0.2691*	*0.2192*	0.044	0.0485
Rain	DJF	0.2786	–0.26	–0.3314	–0.1656	–0.2978
	MAM	–0.1586	−0.1258	–0.1477	−0.0834	−0.0779
	JJA	–0.1557	0.3178	0.1341	−0.1171	0.0289
	SON	0.0067	–0.2192	–0.2127	–0.1828	–0.2215
	YEAR	−0.0464	*–0.0862*	*–0.101*	*–0.1279*	*–0.1534*
Rdur	DJF	0.2693	–0.3045	–0.3391	–0.1714	–0.2955
	MAM	–0.2102	–0.1554	–0.1957	–0.1224	–0.0952
	JJA	–0.2716	0.0509	–0.0667	–0.1392	–0.0046
	SON	0.0289	–0.3017	–0.2605	–0.2202	–0.2175
	YEAR	−0.0568	*–0.2247*	*–0.2231*	*–0.1549*	*–0.168*
SWD	DJF	0.0728	0.1493	0.2682	0.1036	–0.1716
	MAM	0.4995	0.1179	0.1831	0.1788	–0.03
	JJA	0.4934	0.0617	0.1698	0.2033	–0.1081
	SON	0.2903	0.1733	0.2668	0.1623	–0.0342
	YEAR	*0.4053*	*0.0901*	*0.1851*	*0.1697*	−0.0592
TA002	DJF	0.1657	–0.3535	–0.384	–0.0197	–0.2328
	MAM	–0.0927	–0.0837	–0.0587	0.0238	–0.0499
	JJA	0.6796	0.1425	0.3716	0.2681	0.3804
	SON	0.1162	–0.2517	0.0066	0.2163	0.0904
	YEAR	*0.3284*	*–0.1849*	0.01	*0.2045*	*0.15*
TA002max	DJF	0.1072	–0.2263	–0.2462	0.0057	–0.2418
	MAM	0.3141	0.1998	0.3128	0.4247	0.4044
	JJA	0.7373	0.1968	0.4234	0.2921	0.3747
	SON	0.1966	–0.0175	0.2535	0.3422	0.1806
	YEAR	*0.4047*	−0.0168	*0.187*	*0.2679*	*0.2233*
TA002min	DJF	0.1562	–0.3953	–0.4283	–0.0192	–0.1872
	MAM	0.0038	–0.1419	–0.062	0.2603	0.1889
	JJA	0.3213	0.0144	0.1202	0.0917	0.2815
	SON	0.015	–0.3737	–0.1766	0.0797	0.0434
	YEAR	*0.1392*	*–0.2868*	*–0.1593*	*0.0997*	0.081
Td002	DJF	0.0414	–0.2376	–0.3327	–0.0867	–0.1082
	MAM	–0.163	0.0012	0.0106	0.1653	0.2867
	JJA	0.2611	0.1282	0.2301	0.0998	0.5715
	SON	–0.0658	–0.187	–0.007	0.1424	0.1731
	YEAR	0.0367	*–0.1402*	−0.0627	0.0619	*0.2079*
F010	DJF	0.4558	–0.5815	–0.5872	0.071	–0.2567
	MAM	0.1559	–0.4775	–0.5026	–0.0166	–0.3641
	JJA	–0.2383	–0.2836	–0.3272	–0.1039	–0.0579
	SON	0.2235	–0.504	–0.4592	–0.0858	–0.2569
	YEAR	*0.1225*	*–0.4973*	*–0.4806*	−0.0234	*–0.2486*
D010	DJF	0.2893	–0.114	–0.2015	0.0218	–0.194
	MAM	–0.1345	–0.1029	–0.1746	0.0719	–0.1759
	JJA	–0.4293	–0.0467	–0.2335	0.0738	–0.0135
	SON	0.315	–0.2331	–0.2984	–0.0984	–0.1931
	YEAR	−0.0715	*–0.1193*	*–0.2172*	0.0274	*–0.1392*
CC	DJF	0.0084	–0.16	–0.272	–0.0874	0.129
	MAM	–0.4362	–0.1608	–0.2482	–0.1246	–0.0781
	JJA	–0.5611	–0.0902	–0.2226	–0.1238	–0.0106
	SON	–0.2251	–0.285	–0.3341	–0.1157	–0.0551
	YEAR	*–0.3296*	*–0.1757*	*–0.2677*	*–0.1159*	−0.017

Table 4. Overview of the meteorological and air quality variables used in the multiple stepwise regression analysis, for the analysis with (MLR_{METCHE}) or without (MLR_{MET}) the air quality variables as predictors.

Variables	Real-time	Lag24	Lag48 1295
Meteorology			
P0	x	x	x
Rain	x	x	x
SWD	x	x	x
TA002max	x	x	x
TA002min	x	x	x
RH	x	x	x
F010	x	x	x
D010	x	x	x
CC	x	x	x
Environmental			
O_3		x	x
NO		x	x
NO_2		x	x
SO_2		x	x
PM_{10}		x	x

MLR_{MET} (Meteorology variables)

MLR_{METCHE} (all variables)

Table 5. Summary of the model coefficients b, the standardized coefficients β and t-statistic (indicating importance of the variable in the model) for the stepwise multiple regressions MLR_{MET} and MLR_{METCHE} for O_3 and PM_{10}.

			O_3				
	MLR_{MET}				MLR_{METCHE}		
Variable	b	β	t	Variable	b	β	t
(Constant)	–0.601		–1.513	(Constant)	–0.59		–1.597
RH	–0.797	–0.303	–9.593	RH	–0.676	–0.257	–8.561
TA002max	1.523	0.257	6.793	O_3 (lag24)	0.362	0.363	14.728
P0 (lag24)	–0.32	–0.143	–5.889	TA002max (lag24)	1.388	0.233	7.375
SWD	0.06	0.164	5.072	NO_2 (lag24)	–0.165	–0.143	–4.616
TA002max (lag24)	0.817	0.138	4.358	SWD	0.054	0.149	4.965
F010	1.374	0.129	4.794	O_3 (lag48)	–0.119	–0.119	–5.138
DO10 (lag24)	0.19	0.066	2.598	P0 (lag24)	–0.303	–0.133	–5.599
TA002min	–0.652	–0.103	–2.652	TA002max	1.047	0.176	4.905
SWD (lag24)	0.021	0.058	2.199	TA002min (lag24)	–0.525	–0.081	–2.601
D010	0.012	0.056	2.048	F010	1.255	0.115	4.539
				F010 (lag 24)	–1.184	–0.108	–3.846
				D010	0.022	0.076	3.287
				TA002min	–0.576	–0.089	–2.476
				NO (lag24)	–0.023	–0.072	–2.418
Calibration[a]							
R^2	0.37				0.52		
RMSE	14.25				12.75		

			PM_{10}				
	MLR_{MET}				MLR_{METCHE}		
Variable	b	β	t	Variable	b	β	t
(Constant)	1.083		2.492	(Constant)	0.908		2.059
F010	–1.482	–0.182	–4.543	PM_{10} (lag24)	0.343	0.344	9.569
TA002max	1.338	0.294	7.546	NO (lag24)	0.037	0.158	3.85
SWD	–0.048	–0.185	–3.913	RH	0.44	0.232	4.84
F010 (lag24)	–1.286	–0.166	–4.178	TA002max	1.102	0.231	6.024
CC (lag48)	–0.808	–0.124	–3.361	F010 (lag24)	–1.277	–0.156	–3.825
Rain	–75.158	–0.148	–3.938	RH (lag24)	–0.185	–0.097	–2.417
RH	0.322	0.174	3.615	Rain	–65.448	–0.117	–3.226
D010 (lag24)	–0.24	–0.112	–3.01	SWD	–0.032	–0.123	–2.709
Rain (lag24)	–40.81	–0.084	–2.271	NO (lag48)	0.018	0.081	2.225
				D010 (lag24)	–0.016	–0.075	–2.006
Calibration [b]							
R^2	0.25				0.42		
RMSE	11.05				10.12		

[a] Calculated over the period 2001–2004.

[b] Calculated over the period 20 March 2003 to 31 December 2004.

ACPD
8, 21037–21088, 2008

Title Page
Abstract Introduction
Conclusions References
Tables Figures
◀◀ ▶▶
◀ ▶
Back Close
Full Screen / Esc
Printer-friendly Version
Interactive Discussion

Table 6. Validation of the multiple linear regression in 2 modes (MLR-MET and MLR–METCHE) and the Lamb weather type approach in 2 modes (LWT-year and LWT-seas) using the explained variance (R^2), root mean square error (RMSE) and two skill scores (SS_c and SS_p) for O_3 and PM_{10} over the whole measurement period and the validation period 2005–2006.

Calibration (2001–2004)			R^2 (%)			RMSE	SSc	SSp
O_3	Year	DJF	MAM	JJA	SON			
MLR-MET	37.21	29.16	36	50.41	33.64	15.11	94.55	36.28
MLR-METCHE	51.84	50.41	43.56	60.84	44.89	13.33	95.76	50.42
LWT-year	1.21	3.24	3.61	8.41	0*	19.02	91.37	–0.95
LWT-seasonal	12.25	5.29	5.76	22.09	4.84	17.89	92.37	10.68
PM_{10}								
MLR-MET	25	23.04	26.01	28.09	24.01	12.07	72.79	16.88
MLR-METCHE	42.25	31.36	50.41	36	46.24	10.71	86.32	34.51
LWT–year	12.96	12.25	17.64	16	9.61	12.93	80.07	4.59
LWT–seasonal	17.64	17.64	22.09	18.49	16.81	12.58	81.12	9.63
Validation (2005–2006)								
O_3								
MLR-MET	51.84	64	38.44	68.89	26.01	11.27	96.76	9.9
MLR-METCHE	62.41	65.61	51.84	77.44	28.09	10.08	97.41	27.98
LWT-year	4	0.09*	1.69	12.96	0.49*	15.66	93.74	–73.83
LWT-seasonal	20.88	23.04	6.25	29.16	0.16*	14.21	94.84	–43.25
PM_{10}								
MLR-MET	34.81	21.16	51.84	44.89	32.49	6.06	78.3	1.18
MLR-METCHE	36	27.04	46.24	51.84	30.25	6.24	93.35	–4.58
LWT-year	15.8	16.81	24.01	21.16	7.84	6.74	92.24	–22.17
LWT-seasonal	23.29	22.09	27.04	24.01	20.25	6.44	92.93	–11.3

* insignificant at the 90% confidence interval.

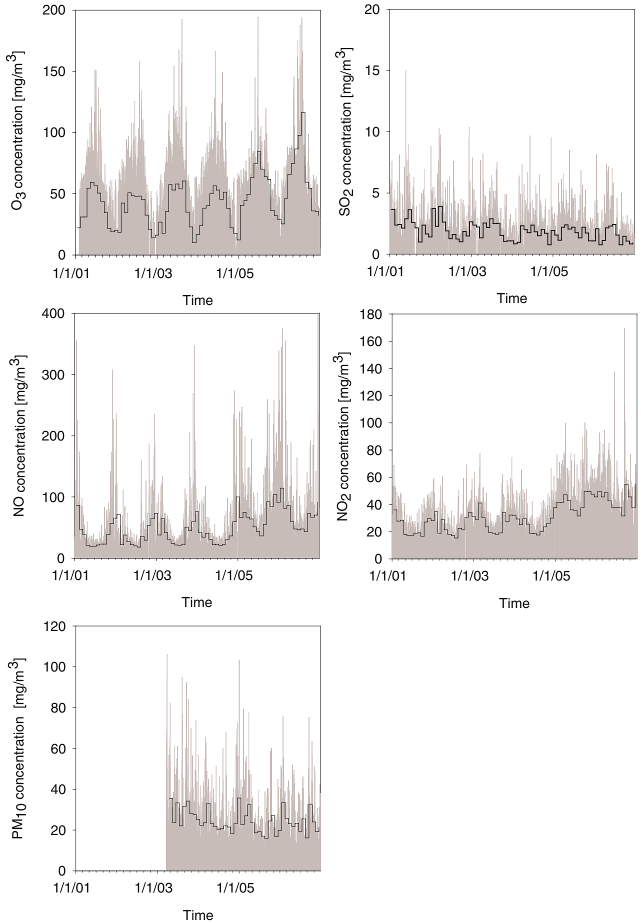

Fig. 1. Time series of daily (grey bars) and monthly mean (black line) values for surface O_3, NO, NO_2 and SO_2 measured at Cabauw between 2001–2006 and for PM_{10} measured at Zegveld-Oude Meije between March 2003–2006.

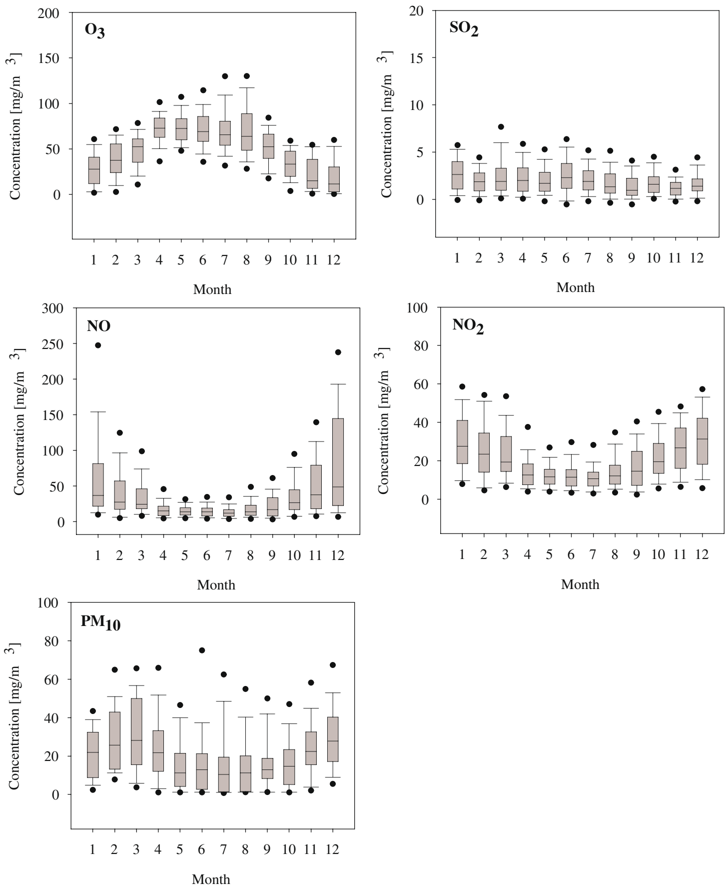

Fig. 2. Box plots showing distribution of O_3, NO, NO_2, SO_2 and PM_{10} concentrations per month. The box and whiskers present the median, the first and third quartiles, the minimum and maximum value and possible outliers.

ACPD

8, 21037–21088, 2008

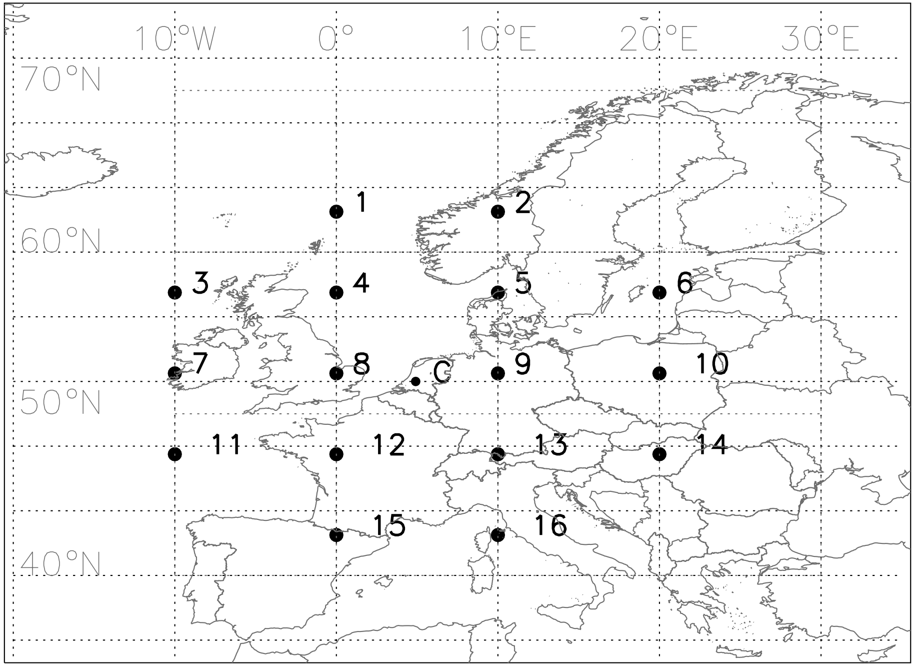

Fig. 3. Location of the 5°×10° SLP grid used, with 16 point centered over the Benelux. "C" denotes the location of the Cabauw measurement station and the grid center.

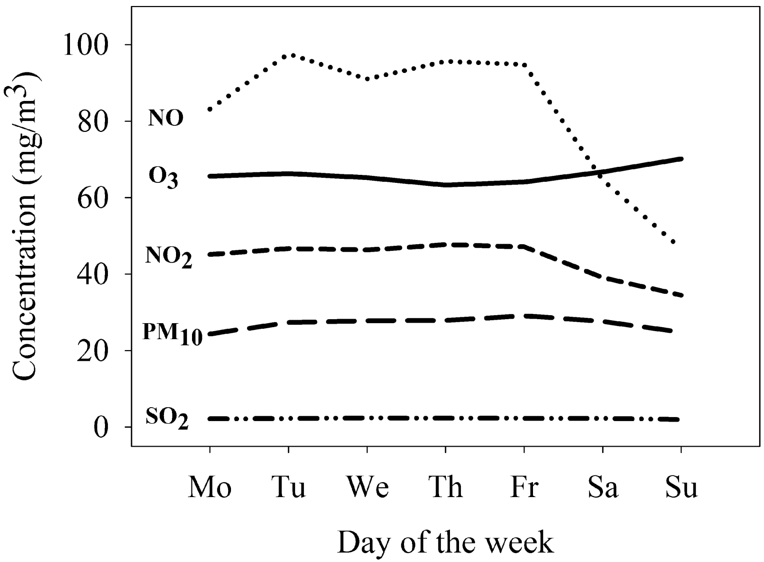

Fig. 4. Weekly cycles for O_3, NO, NO_2 and SO_2 and PM_{10} concentrations derived from the measurement station of Cabauw.

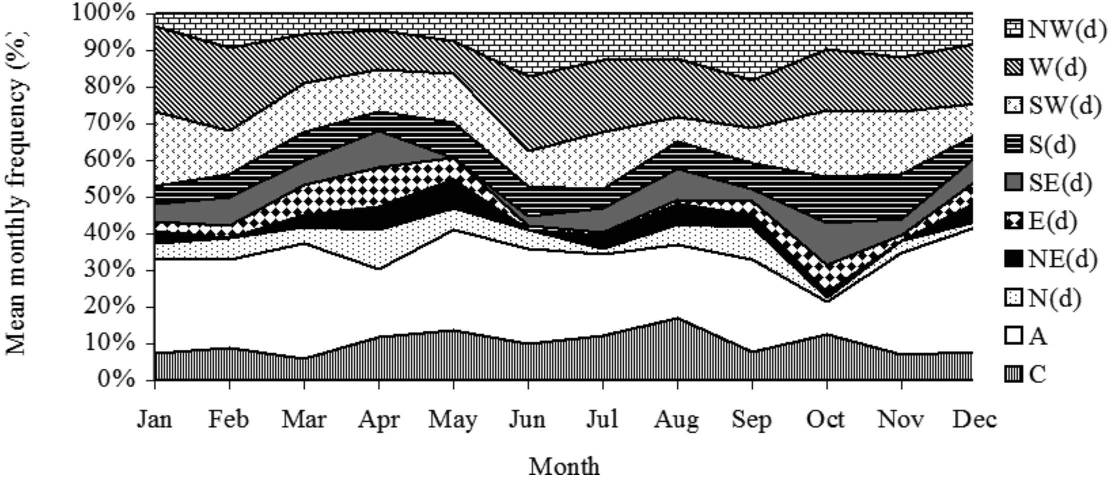

Fig. 5. Monthly mean frequencies of Lamb Weather Types over the period 2001–2004.

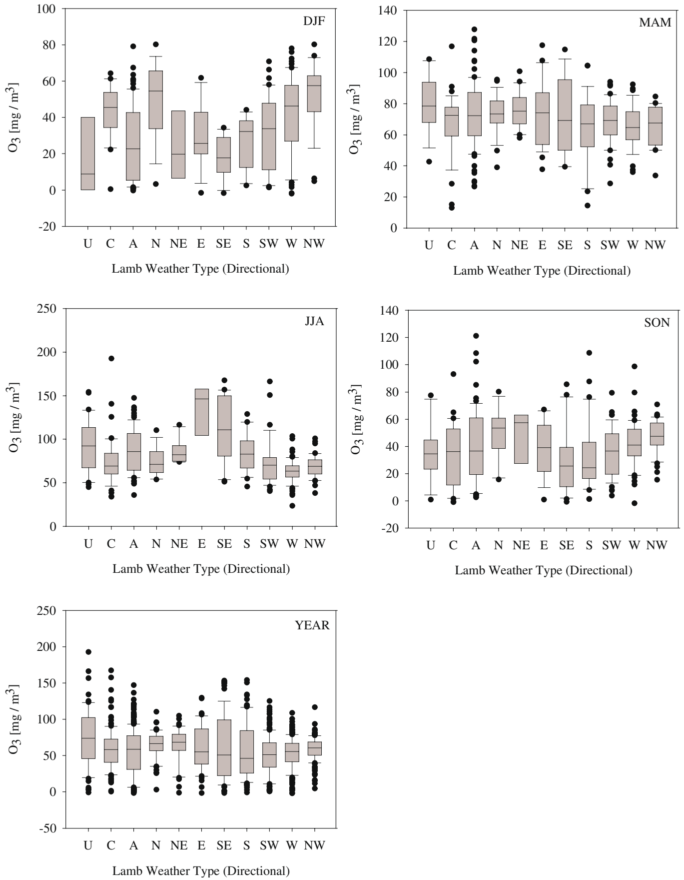

Fig. 6. Box – Whiskers plots with the concentrations of O_3 according to the Lamb weather type classes per season and year, averaged over the period 2001–2004. The box and whiskers present the median, the first and third quartiles, the minimum and maximum value and possible outliers.

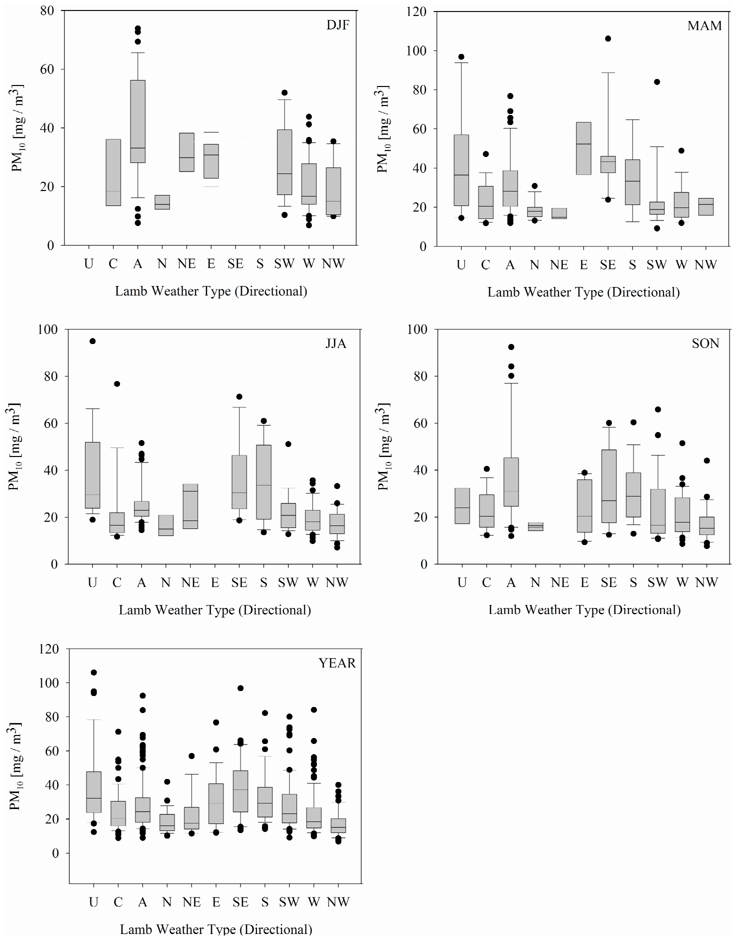

Fig. 7. As in Fig. 6, but for PM_{10}.

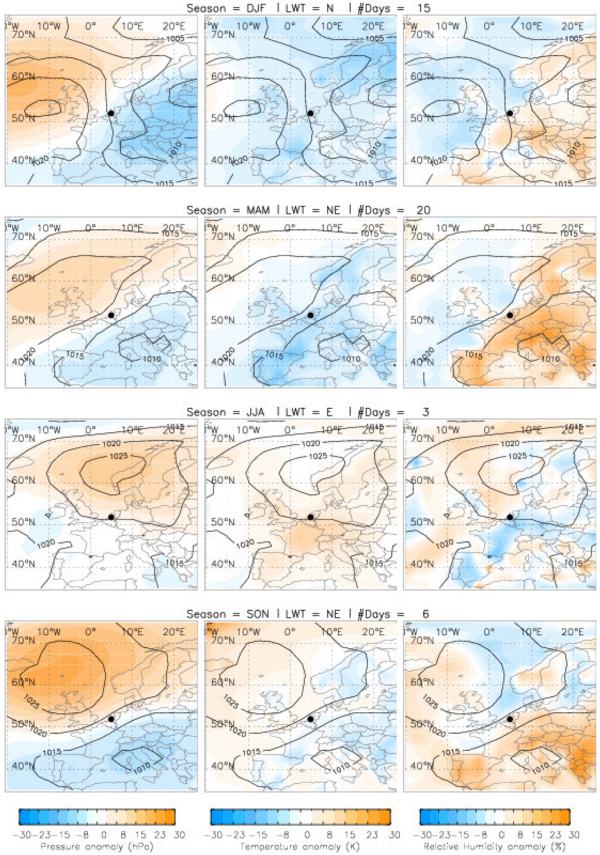

Fig. 8. Mean surface pressure fields (in hPa) for the circulation type in each season characterized by the highest median O_3 concentration for the period 2001–2004. Shaded colours show the pressure anomalies (left panels), 2m temperature anomalies (middle panels) and relative humidity anomalies (right panels) from the long-term mean (1971–2000). The full dot refers to the Cabauw measurement location.

ACPD

8, 21037–21088, 2008

ACPD

8, 21037–21088, 2008

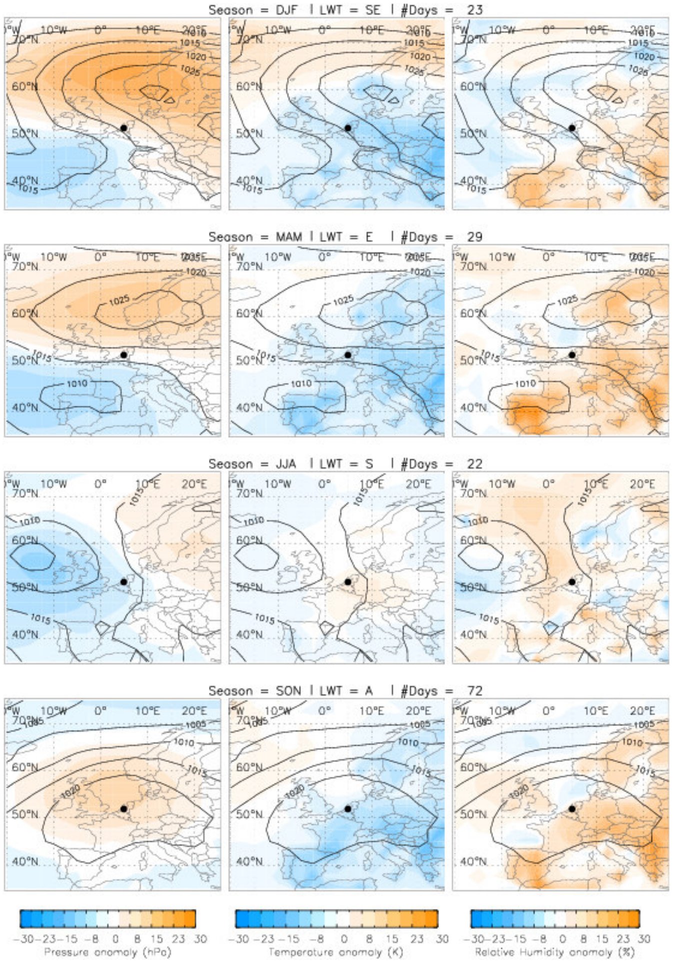

Fig. 9. Same as Fig. 8, but for PM_{10}.